Research Article

Research on the Preparation and Mechanism of the Organic Montmorillonite and Its Application in Drilling Fluid

Xiaolong Wang,[1,2] Baolin Liu,[1,2] and Peizhi Yu[1]

[1]*School of Engineering and Technology, China University of Geosciences, Beijing 100083, China*
[2]*Key Laboratory on Deep Geo-Drilling Technology of the Ministry of Land and Resources, China University of Geosciences, Beijing 100083, China*

Correspondence should be addressed to Baolin Liu; lbaolin@cugb.edu.cn

The study focused on the relation of structure, property, and application of composite prepared by organic cation intercalated montmorillonite (Mt). Herein a new kind of green and steady ionic liquid, 1-hexadecyl-3-methylimidazolium chloride monohydrate (C_{12}mimCl), was chosen as the intercalated agent. This study used molecular dynamics (MD) modeling to examine the interlayer microstructures of montmorillonite intercalated with C_{12}mimCl. The C_{12}mimCl intercalation was relatively fast with a large rate constant. The process was affected by the initial concentration of the solution; the basal spacing increased to 2.08 nm after intercalation. The coordination of electrostatic interaction and hydrogen bonding expelled water molecules out of the clay gallery and bound the layer together, which led to the dehydration of clay. The intercalation of C_{12}minCl into Mt interlayer space affected rheology of the system and improved various properties. This organic clay composite was environmentally friendly and could be used in drilling fluid system. These models provided insights into the prediction of synthesized organic cationic-clay microstructure and guidelines for relevant engineering applications.

1. Introduction

Montmorillonites (Mts) are clay minerals with regular layer structure composed of octahedral sheet between two tetrahedral sheets. Intercalating organic and inorganic species into layered host materials has drawn researchers' increasing interests. It is an effective way to construct ordered inorganic-organic and inorganic-inorganic assemblies with unique microstructures and properties [1, 2]. The montmorillonite's group of clay minerals provides attractive features, including large surface area, swelling behavior, adsorption, and ion exchange [3, 4]. The intercalated single layer nanosized Mt particles (0.6–1 nm in width) are ideal dispersing additives for the synthesis of organic-inorganic hybrid nanocomposites to enhance mechanical, thermal, and chemical stabilities. Montmorillonites have been extensively used as the host materials and in other possible ways because of their attractive properties and ability to accommodate various kinds of organic and inorganic guest species [5].

Numerous reports about studies and applications on organics modified Mt have been published, while few work has been reported on the application of geological drilling fluids [6, 7]. Water-based drilling fluid system is composed of clay, water, and treatment agent. Mt is a significant mineral material to adjust rheology and fluid loss of drilling fluid. As a drilling fluid material, organic Mt has excellent rheology and viscosity [8]. The drilling slurry, mainly composed of Mt, is used for protecting wall, clearing away cuttings, and cooling drill.

In oil-well drilling, bentonite is added in drilling fluids for viscosity control, to aid the transfer of cuttings from the bottom of the well to the surface, and for filtration control to prevent filtration of drilling fluids into the pores of productive for mations [9]. Compared to water-based drilling fluid, oil-based drilling fluid has many inherent advantages, including excellent clay inhibition, wellbore stability, lubricity, antiaccretion property, temperature stability, tolerance to contamination, and corrosion protection [6]. The high clay

solids content in drilling fluid has several adverse effects: (1) greatly reduces the rate of penetration [7]; (2) increased chances of differential sticking; and (3) is the major cause of excessive torque and drag [10]. Thus, low bentonite content is desired to control the total amount of solids. At low concentration, bentonite clay is unable to provide satisfactory rheological properties required for optimum performance in oil-well drilling. Hence, polymers are added to achieve the desired result. In addition, if dispersion and rheological property of organic Mt are poor, highly flocculating and its presence in the mud can adversely affect rheology and filtration control [8].

Most commonly, Na-montmorillonite is used as the base clay and its sodium cations can be exchanged with quaternary ammonium cations [11, 12]. QAC-coated montmorillonite exhibits higher zeta potential [13], enhanced strength, lower compressibility, and stronger retention of organic compounds [14, 15] in the environment, yielding a variety of potential applications in the waste containment, landfill liners, and slurry walls [16–19]. Because of low saturated vapor pressure of quaternary ammonium surfactants and potential toxicity to environment, the application of surfactants is restricted.

Ionic liquids are composed solely of ions. Since they are nonvolatile, nonflammable, highly conductive, and chemically and thermally stable, they can be used in catalysis, electrochemistry extraction and other technological applications [20]. This new technology, so-called supported ionic liquid phase (SILP) catalysis, combines the advantages of ionic liquids with those of a heterogeneous material supported on the solid phase, resulting in materials of low toxicity, which are environmentally benign and have a wide range of applications [21–24]. Ionic liquid modified clays have recently been paid attention to due to their unique properties, such as negligible vapor pressure, no flammability, and electrical conductivity. Ionic liquids are all favorable for fabricating the inorganic clay-organic intercalation compounds with a high thermal stability or compositing materials with an improved flame retardant property.

In the present work, $C_{12}mimCl$ is used as intercalant agent for montmorillonite. X-ray diffraction (XRD) technique is used to study properties of the modified montmorillonite. The cation exchange capacity of modified montmorillonite is also measured and the obtained result proves that the intercalation is successful. Based on these experimental results, molecular dynamics simulation on intercalation process of using $C_{12}mimCl$ as intercalant agent for montmorillonite is conducted.

2. Materials and Methods

2.1. Materials. The montmorillonite (Mt) used was obtained from the Clay Mineral Repositories in Purdue University (West Lafayette, IN) without further purification. It had a chemical formula of $(Ca_{0.12} Na_{0.32} K_{0.05})[Al_{3.01} Fe(III)_{0.41} Mg_{0.54}][Si_{7.98} Al_{0.02}]O_{20}(OH)_4$, a cation exchange capacity (CEC) of $85 \pm 3\,mmol_c/100\,g$ [25], a layer charge of $0.32\,eq/mol$ per $(Si, Al)_4O_{10}$ [26], an external surface area

(ESA) of $23\,m^2/g$ [27], and a mean particle size of $3.2\,\mu m$ with a d_{25} to d_{75} in the range of $3\sim10\,\mu m$.

The 1-dodecyl-3-methylimidazolium Chloride monohydrate (CAS#: 114569-84-5, $C_{12}mimCl$), was obtained from Shanghai Darui Fine Chemical Co. Ltd. (Shanghai, China). They had pKa values of 7.08 ± 0.1, calculated on ACD online services website, due to protonation of both nitrogen atoms. When the solutions' pH value was less than 5.2, $C_{12}mimCl$ exists as $C_{12}mimH^+$; when pH value was between 5.2 and 9.2, its existence would change to monovalent cation and neutral molecule, and when pH value was above 9.2, it would be of nonion form.

2.2. Methods. The initial $C_{12}mimCl$ concentrations varied from 10 to 5000 mg/L for the adsorption isotherm study. The mass of Mt used was 0.2 g while the volume of solution used was 25 mL for all studies except the kinetic study. The solid and solution were combined in each 50 mL centrifuge tube and shaken for 2 h at 150 rpm. All experiments, except kinetic experiment, were performed at room temperature. After the mixtures were centrifuged at 10000 rpm for 20 min, the supernatants were filtered through $0.22\,\mu m$ syringe filters before being analyzed for equilibrium $C_{12}mimCl$ concentrations.

The equilibrium $C_{12}mimCl$ concentrations were analyzed with a UV-Vis spectrophotometer (Model T6 New Century 1650, made by General Instrument, Inc. LLT, Beijing China) at the wavelength of 210 nm, corresponding to its maximal absorbance. Calibrations were made using standards of 10, 20, 30, 40, 50, and 60 mg/L with a regression coefficient of 0.9998. The amount of $C_{12}mimCl$ adsorbed was calculated from the difference between the initial and final concentrations.

Powder XRD analyses were performed on a Rigaku D/max-III A diffractometer (Tokyo, Japan) with a Ni-filtered CuKα radiation at 30 kV and 20 mA. Orientated samples were scanned from $3°$ to $10°$ at $2°$/min with a scanning step of $0.01°$. The changes in the XRD peak positions reflected the hydrated size of the metal cations in the interlayer space of Mt.

FTIR spectra of samples were collected on a Nicolet-560 spectrometer (Thermal Nicolet Co., USA) from 400 to $4000\,cm^{-1}$ with a nominal resolution of $4\,cm^{-1}$. For each spectrum 16 runs were collected and averaged. The Mt specimens were prepared by adding approximately 1% of the sample powder to dry KBr powder.

The water contact angle (CA) and sliding angle (SA) were measured at ambient temperature with a SL200B apparatus from ZhongChen Digital Equipment Co. Ltd., Shanghai. The CAs reported here were the mean values measured with ca. $5\,\mu L$ water droplets at five different positions on each sample. The samples used were shaped into a circle piece using a tablet machine under 15 Mpa at room temperature.

Thixotropic loop area of the composite material was tested by Rotational Rheometer (RotoVisco1), Thermo Fisher Scientific Company, and viscosity was tested by Digital Viscometer (SNB-3), Shanghai Jingtai Electronic Instrument Co., Ltd. Thixotropy meaned gels or fluids get thin or less viscous when stirred or under some mechanical action and back to thick or static condition after being placed for a certain time. At a certain shear speed, the shear stress acting

on a thixotropic system lowered as time was getting longer. The experiment used reading value of Viscometer after 10 s of start as the viscosity of composite material, shearing and recovering both taking for 3 min. It was solution of C_{12}-Mt, Xylene as solvent, and the concentration was 3%. Thixotropic ring method was used for recording viscosity of paint successively during speed of viscometer which increased (shearing) then decreased (recovering), drawn into a reciprocating curve. Flow curve of composite material was determined by HAAKE RotoVisco1 rheometer, with shear rate range of upstream $0\,s^{-1}$~$200\,s^{-1}$, downstream $200\,s^{-1}$~$0\,s^{-1}$, up and down each 3 min, thermostat 25°C. Automatically fit the measured data by the computer, drew the shear stress and shear rate curve, integral calculated the area of thixotropic loop between ascending and descending curve.

2.3. Computation Details. Molecular simulation was performed under the module "CASTEP" of Materials Studio 6.0 software to investigate the sorption sites of Na^+ on Mt. The primitive unit cell of Mt was optimized with the generalized gradient approximation (GGA) for the exchange-correlation potential (PW91) which was appropriate for the relatively weak interactions present in the models studied. The resulting primitive unit cell was characterized by the parameters $a = 15.540\,\text{Å}$, $b = 17.940\,\text{Å}$, $c = 12.56\,\text{Å}$, and $\alpha = \gamma = 90°$, $\beta = 99°$. Based on the primitive unit cell, a series of $(3 \times 2 \times 1)$ super cells were built.

In order to investigate the intercalated mechanism of $C_{12}mim^+$ in pure Mt layer, simulated annealing algorithm was used to perform canonical Monte Carlo (MC) simulation with $C_{12}mim^+$ simulated as adsorbate on the layer of pure Mt. The number of cycles was 3 and the steps of one cycle was 10^6 a representative part of the interface devoid of any arbitrary boundary effects. Based on the structure of the preferential adsorption model of $C_{12}mim^+$ in the layer of Mt predicted by MC calculation, GGA-PW91 was used to optimize the structure again and to predict the interaction energy between $C_{12}mim^+$ and Mt layer to a greater accuracy. All of the GGA-PW91 calculations were performed using a double numerical plus polarization function (DNP) as basis set and DFT-D correction. So all calculations, the heavy atoms of Mt were frozen, whereas the hydrogen of Mt, cationic molecules was fully relaxed.

3. Results and Discussion

3.1. Amount of $C_{12}mimCl$ Intercalated into the Mt. The reaction time (Figure 1(a)) and initial concentration (Figure 1(b)) of solution were two important factors affecting Mt's intercalation by $C_{12}mimCl$. It was a rapid process of organic cations intercalated into Mts; half of maximum amount of intercalation could be reached in 5 min, while full maximum amount of intercalation would be achieved in 20 min. It was similar to organic cations adsorbed or intercalated clay minerals. Organic cations intercalating Mt were mainly of cations exchange in accordance with the second-order kinetic equation.

The kinetic study aimed to investigate the time needed to reach equilibrium for intercalation with $C_{12}mimCl$ so that

future studies could be unified into a fixed time by which equilibrium would be established. Intercalation of $C_{12}mimCl$ into Mt was instantaneous (Figure 1(a)). The experiment data were fitted to several kinetic models and the pseudo-second-order kinetic was confirmed by fitting t/q_t (where q_t was amount of $C_{12}mimCl$ removed, t denotes time) into a straight line [28]. The coefficient of determination r^2 was 0.999 for both Mts. For Mt intercalated with $C_{12}mimCl$, an initial rate of 132 mmol/g h, a rate constant of 254 g/mmol h, and q_e, the amount of $C_{12}mimCl$ adsorbed at equilibrium, of 0.21 mmol/g were obtained. The instantaneous Mt intercalation with $C_{12}mimCl$ suggested a great affinity of $C_{12}mimCl$ for Mt surfaces. Thus, for the intercalation with cationic drugs, such as $C_{12}mimCl$ from water, swelling clays-like Mts offered a great advantage due to their larger initial rate, rate constants, and higher capacity.

Initial concentration of solution had a profound influence on the amount of intercalation (Figure 1(b)). The intercalation amount of $C_{12}minCl$ to Mt increased as the concentration of solution increased. When the concentration of $C_{12}minCl$ was 10~2000 mg/L, the rate of intercalation increased sharply. When concentration was above 2000 mg/L, it increased slowly. After intercalation reached the balance point at 5000 mg/L concentration, the intercalation amount of $C_{12}minCl$ to Mt did not change. At last, maximum amount of intercalation was 0.75 mmol/g. As the basal spacing increased because of intercalation, it followed that hydrophobic and repel force among alkyl chains of organic cations cause organic cations to intercalate into layers of Mt. The quantity of the organic cations entered into Mt's layer was larger than that was swapped out. Klebow and Meleshyn discussed this problem in one of their papers [29], and the extra charge could be offset by the absorption of the negative ion from the solution on the surface of montmorillonite [30, 31].

3.2. Performance of $C_{12}mimCl$ Intercalated into the Mt. With the ion exchange of the sodium ion for the $C_{12}mim^+$, expansion of the Na-Mt layers occurred. This expansion was readily measured by XRD. Modified by the $C_{12}mimCl$, the basal spacing of the Mt was expanded; the basal and basal spacing were observed for the different clays (Figure 2). The trend for the basal spacing d_{001} was the same as that in the basal spacing. The differences between the organo-Mt were due to the different incorporation and arrangement of the surfactants.

$C_{12}mimCl$ exchanged Na^+ ion in Na-Mt interlayer, leading to obvious increase in d_{001} value of Mt. The raw Mt and Mt equilibrated with 1000 mg/L of $C_{12}mimCl$ were further analyzed from 3° to 10°. The information of $C_{12}mimCl$ intercalating towards Mt could be obtained more directly by examining the change of basal spaces from XRD results (Figure 2(a)). Mt's basal space was 14.34~14.59 Å under the intercalating time ranging from 5 min to 18 h, with no obvious difference. This result demonstrated that the intercalation balance under this concentration could be reached in 5 min, which was consistent with the experiment data.

The basal space for $C_{12}mimCl$ intercalated Mt would change according to the change in amount of $C_{12}mimCl$ and
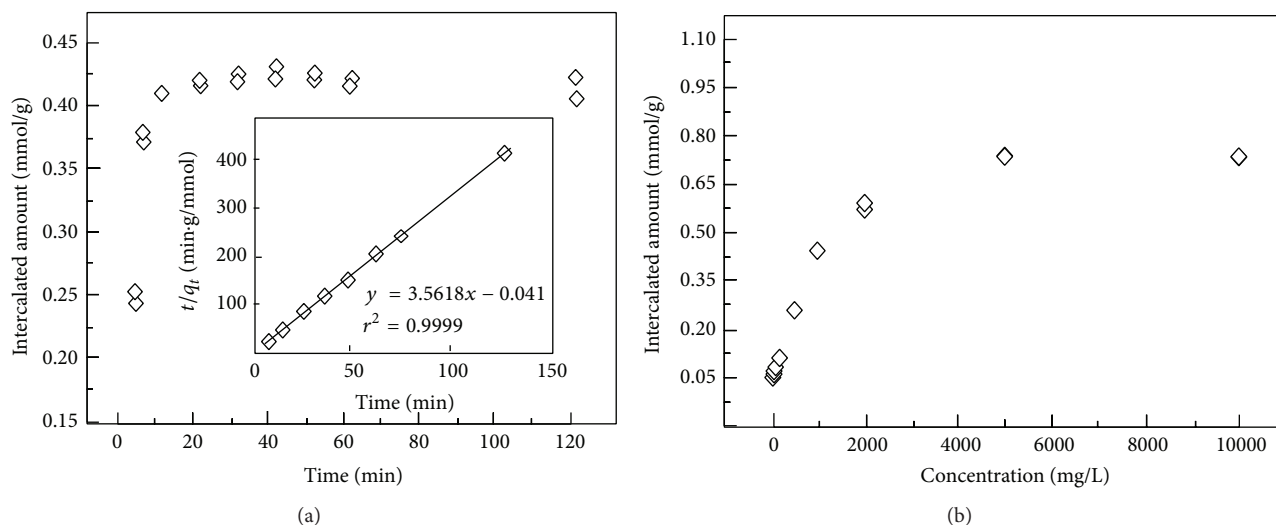
FIGURE 1: Kinetics of C_{12}mimCl intercalated into Mt (a). The solid line is pseudo-second-order fit to the observed data. Inserts are plot of t/q_t against t for Mt. Effect of C_{12}mimCl concentration on intercalated quantities (b).
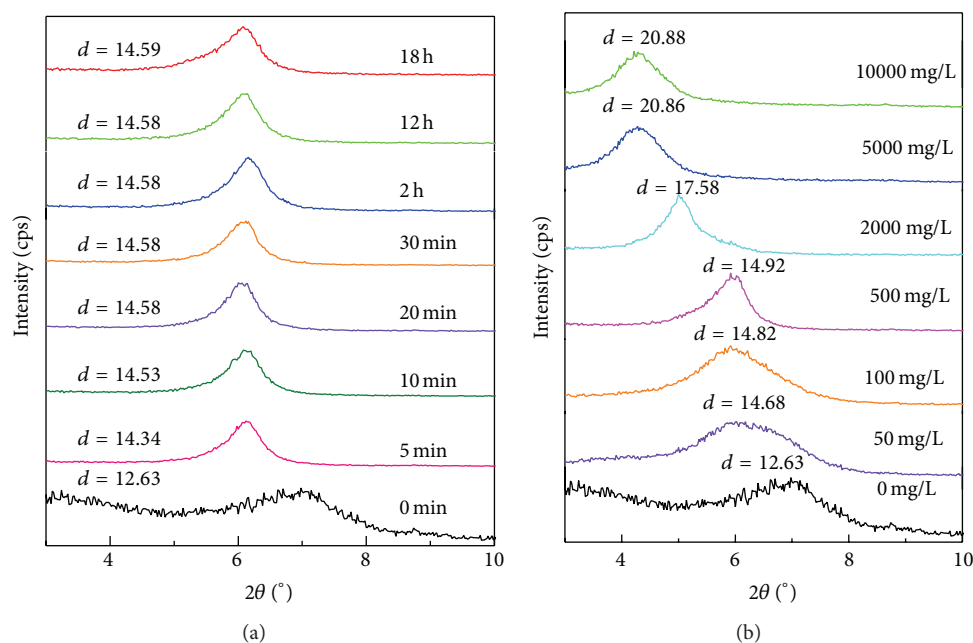

FIGURE 2: X-ray diffraction patterns of Mt before and after equilibrated at different contact time (a) and initial concentrations (mg/L) (b) of C_{12}mimCl (d/Å).

the way they arranged themselves in the interlayer. The XRD results (Figure 2(b)) showed that the d_{001} value remained at 14.92 Å as the initial concentration changes from 10 mg/L to 500 mg/L, which was larger than unmodified Mt by 2 Å. As the initial concentration increased, the amount of C_{12}mimCl intercalated into Mt increased and its configuration in the interlayer changed as well. At concentration of 5000 mg/L, basal spacing of Mt expanded to 20.88 Å. The basal spacing reached the maximal value and would not change as the concentration increases.

Vibrational spectroscopy had been extensively used to probe the local environments of cationic surfactants in the basal space of Mt [32–35]. FTIR studies had revealed detailed correlation of the spectra with structural features. The position, splitting, and intensities of methylene stretching modes in the FTIR spectra had been acknowledged as useful indices in the study of conformation of alkyl chain assemblies [36–39].

FTIR spectra of before and after C_{12}mimCl intercalated Mt displayed formation and breakage of chemical bond were
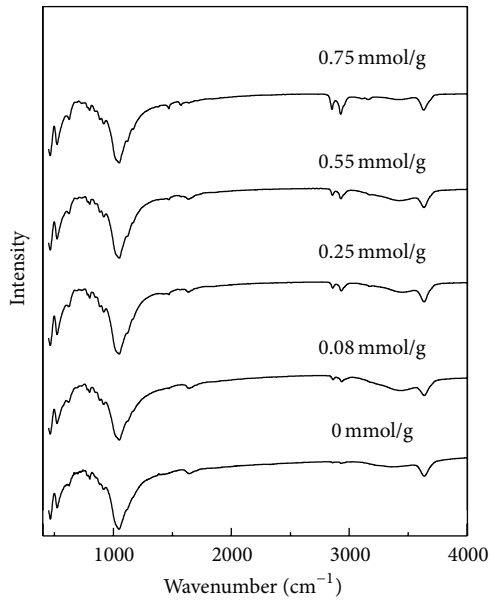
Figure 3: FTIR analyses of Mt intercalated with $C_{12}mimCl$.

Table 1: Performance parameters of Mt and organic Mt.

Concentration of $C_{12}mimCl$ (mg/L)	Viscosity curve	Contact angle pattern (°)	Viscosity (mPa·s)	d_{001} (Å)
0 mg/L	—	48	—	12.63
50 mg/L	25	54	22.8	14.68
100 mg/L	36	59	29.0	14.82
500 mg/L	44	63	36.3	14.92
2000 mg/L	51	67	43.4	17.58
5000 mg/L	58	71	49.3	20.86
10000 mg/L	58	72	49.8	20.88

clear in Figure 3. Only one variation in 2850~3000 cm^{-1} was detected when scanning in 450–4000 cm^{-1}. The FTIR absorption bands at 3000 to 2850 cm^{-1} were attributed to the symmetric CH$_2$ stretching (v_s(CH$_2$)) and antisymmetric (v_{as}(CH$_2$)) modes. It had been well established that the frequencies of the CH$_2$ stretching bands of hydrocarbon chains were extremely sensitive to the gauche/trans conformer ratio of the hydrocarbon chains [32, 39]. Only when the chains were highly ordered (all-trans), the narrow absorption bands appeared around 2850~2885 cm^{-1} and 2921~2965 cm^{-1} in the infrared spectrum. 1450–1480 cm^{-1} and 1550–1600 cm^{-1} were C=C stretching vibration of absorption valley. We explain that $C_{12}mim^+$ has been intercalated into the Mt layers. If conformational disorder was included in the chains, their frequencies might shift upward or downward, depending upon the average content of gauche conformers [34].

The contact angle of a material could probe whether it was hydrophobic or hydrophilic: When the contact angle ≤ 90°, it was hydrophilic. And when contact angle ≥ 90°, it was hydrophobic. For Mt, the contact angle increased as the amount of intercalation increased. The contact angle of Mt is 48° before being intercalated. As the concentrations of the solution were 50, 100, 500, and 10000 mg/L, the contact angle was 54°, 59°, 63°, and 72°, respectively (Figure 4).

To clay used in drilling fluid, good thixotropy and rheology were necessary. Thixotropy of Mt and organic modified Mt were compared to study application performance of Mt. Table 1 showed parameters of structure and property of $C_{12}minCl$ modified Mt. It could be found that after being modified by $C_{12}minCl$, d_{001} value of Mt increased from 1.26 nm to 2.08 nm and colloidal rate increased from 5 to 46. The increase in thixotropy was performed as increasing thixotropic ring area and thixotropic index. Because $C_{12}minCl$ entered interlayer region of Mt, Mts with expanded interlayers were easier to swell than unintercalated

Mt raw material. At stirring condition of drilling fluid, a "house of cards" structure had been formed by layers and it provided better thixotropy. Increasing contact angle indicated increased organic degree of Mt (lipophilicity-hydrophobicity). Mt material was more compatible to drilling fluid at a higher organic degree, whose thixotropy was easier to be utilized. As intercalation amount of $C_{12}minCl$ to Mt increased, basal spacing, thixotropic index, and thixotropic ring area of Mt increased and it had a better thixotropy. Figure 5 was thixotropic curve of organic Mt as concentration of $C_{12}minCl$ increased. As intercalation amount of $C_{12}minCl$ increased, the curve became smoother and enclosed area was bigger than unmodified Mt. In addition, viscosity of organic Mt was another important parameter to express performance of drilling fluid system. Viscosity of organic Mt increased as organic degree increased, but in application it should be kept about 40~60 MPa·s, for excessive viscosity had an impact on mobility. Therefore, viscosity, rheology, contact angle, and thixotropic ring area should be considered for the application of Mt in drilling fluid. In conclusion, various performances of Mt had been improved after $C_{12}minCl$ modification and it could be used as an environmentally friendly and effective composition of drilling fluid [23, 24, 40].

3.3. Molecular Dynamics. The research simulated the interlayer $C_{12}mimCl$ ion's interaction with Mt layers, amount of intercalation and its arrangement. After working out size of unit cell and basal spacing from the amount of intercalation, it could be calculated that numbers of intercalated $C_{12}mimCl$ is 4 (Figure 6). Their arrangements were as follows: The $C_{12}mim^+$ molecules arrange in bilayers parallel to Mt layers. The obtained results were in good agreement with the experiment. When $C_{12}mimCl$ was located in interlayer, N$^+$ of pentagonal ring was close to oxygen of silicon-oxygen tetrahedron in Mt layer and the alkyl chain of another $C_{12}mimCl$ and forms a cross-pattern. As electrostatic field of N$^+$ acted on alkyl chain of $C_{12}mimCl$, the amount of intercalation exceeds CEC value of Mt. The amount of $C_{12}mimCl$ intercalating into Mt reaches 1.2 times of CEC value of Mt.

The energies before and after $C_{12}mimCl$ intercalating Mt were different due to the vector sum of the interaction force, which existed among organic cations themselves, organic cations, and layers and determines the final energy. In addition, the bond length and angle of organic cation to oxygen hexagonal ring of silicon-oxygen tetrahedron in Mt layer
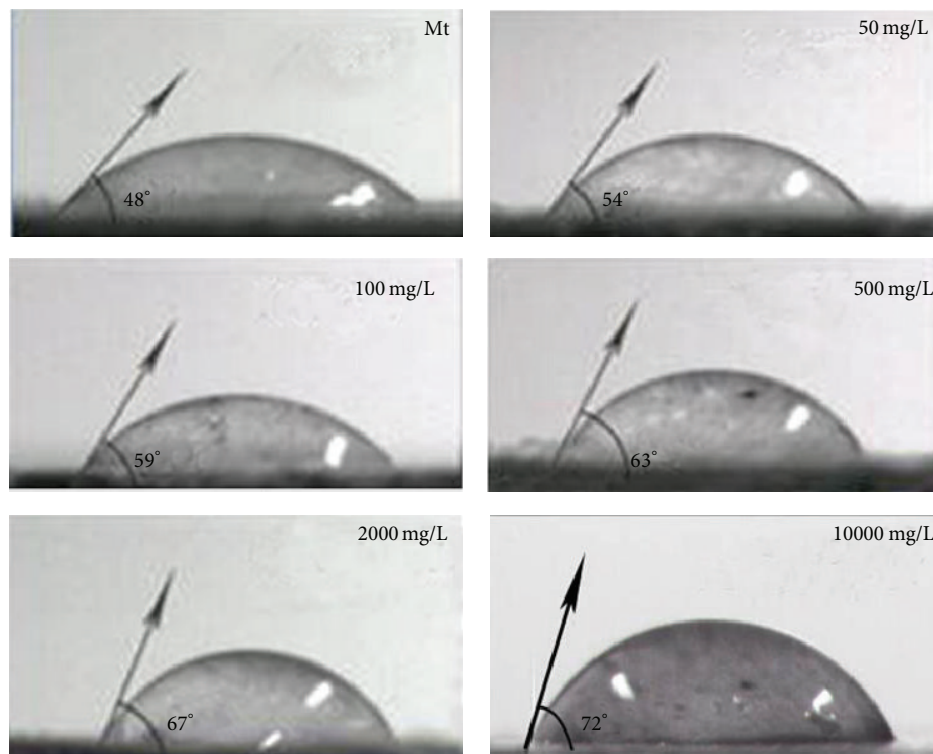
FIGURE 4: Contact angle pattern of Na-Mt and the organic Mt samples.

affected the arrangement of $C_{12}mim^+$ ions in Mt interlayer. In the simulation process, two $C_{12}mimCl$ were put into interlayer without H_2O, in consideration of the interaction between organic cations and layers.

The headgroup of the $C_{12}mimCl$, which carried the positive charge of the organic cation, was attracted to the clay surface via electrostatic forces ($C_{12}mimCl$ head and mineral interface were shown in Figure 7). Figure 7 of the clay surface oxygen versus $C_{12}mim^+$ nitrogen indicates that the minimum distance of $C_{12}mim^+$ nitrogen to the surface oxygen was 3.121 Å. The minimum distances of H (-CH$_3$) in $C_{12}mim^+$ to O in silica-tetrahedron were 2.071 Å, which were smaller than 2.5 Å. It should be addressed that the interaction force of H and O in $C_{12}mim^+$ was bigger than that of N^+ and O. The N^+ atom of $C_{12}mimCl$ molecule played the most dominant role in the stabilization and the localization of the molecule in the basal space. Take the intercalating mode of N-CH$_3$ group form hydrogen bonds with nearby two upright -N-O groups of the tetrahedron Si sheet with the O-N-O angles of 45.18° (Figure 7). In contrast to previous observations for the R-N^+-CH$_2$ group, no hydrogen bond was formed between the N^+ methyl group (CH$_3$) and the clay surface oxygen, which also indicated that the $C_{12}mim^+$ headgroup could have lateral rearrangement across cavities [41]. However, comparing the N-CH$_3$ head group with carbon tails, the simulation results indicated that the $C_{12}mim^+$ head could be considered as an immobile phase near the clay surface, when compared with the nonpolar carbon tails, which was in agreement with what had been reported by Heinz et al. [42].

In Section 3.1, it had been established in the contact angle discussion that Mt became hydrophobic after being intercalated with $C_{12}mim^+$ and there were no free water molecules in the interlayer after drying process at low temperature. However, the intercalation of Mt with organic cations occurred in solution, which meant that water molecules could enter the interlayer of Mt and interacted with $C_{12}mim^+$ (Figure 8). Interaction between $C_{12}mim^+$ and water deserved further discussion. In order to prove the theory above, a simulation was conducted. To simplify the model, one $C_{12}mim^+$ with 10 water molecules around were arranged in the interlayer of Mt to simulate the state in solution and to discuss the interaction between $C_{12}mim^+$ and water molecules. The closest distance between N^+ in $C_{12}mim^+$ and the oxygen in silicon-oxygen tetrahedron was 4.614 Å, so $C_{12}mim^+$ could not form chemical bond with oxygen in silicon-oxygen tetrahedron. The interaction between $C_{12}mim^+$ and water molecules was also weak because the closest distance between N^+ in $C_{12}mim^+$ and the oxygen in water molecules was 4.058 Å. The distance between alkyl chains in $C_{12}mim^+$ and oxygen in water was more than 5 Å, indicating totally hydrophobic. Therefore, in organic environment, intercalation with organic cations could change the interlayer of Mt from hydrophobic to hydrophilic.

4. Conclusions

$C_{12}mimCl$ had been successfully intercalated into the interlayer of Mt. Molecular dynamic simulation was used to study the effect of initial concentration and time on the
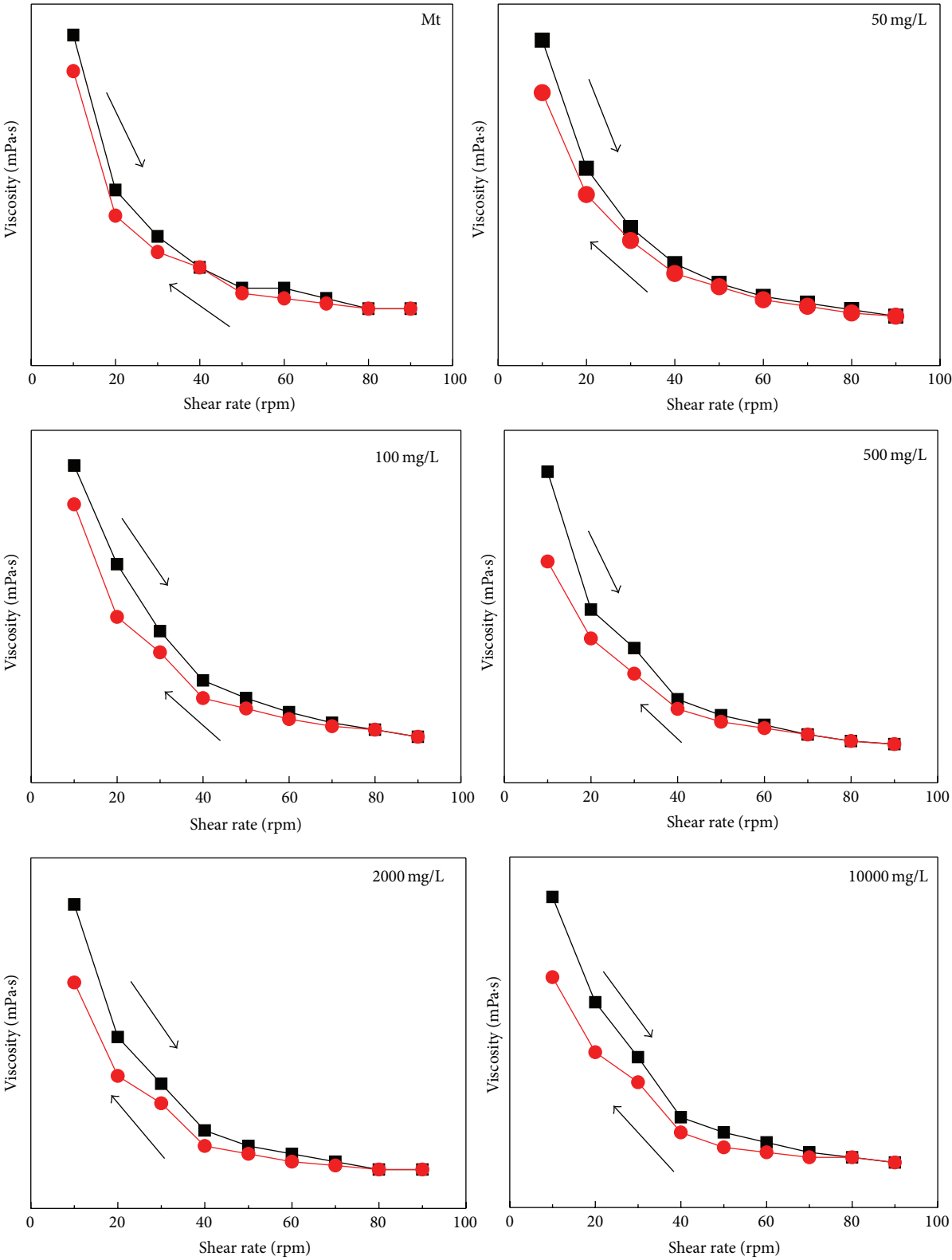
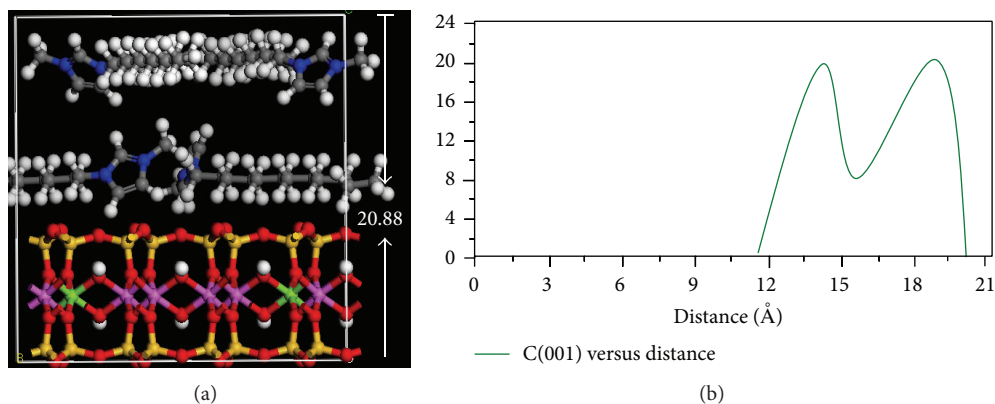Figure 5: Viscosity curve of Mt and organic Mt.

(a)

(b)

FIGURE 6: Molecular dynamic simulation of intercalation of C_{12}mimCl into Mt (a). C_{12}mimCl molecules (b) from the origin. For all species, C = gray, N = blue, H = white, O = red, Si = yellow, Al = purple, and Mg = green.
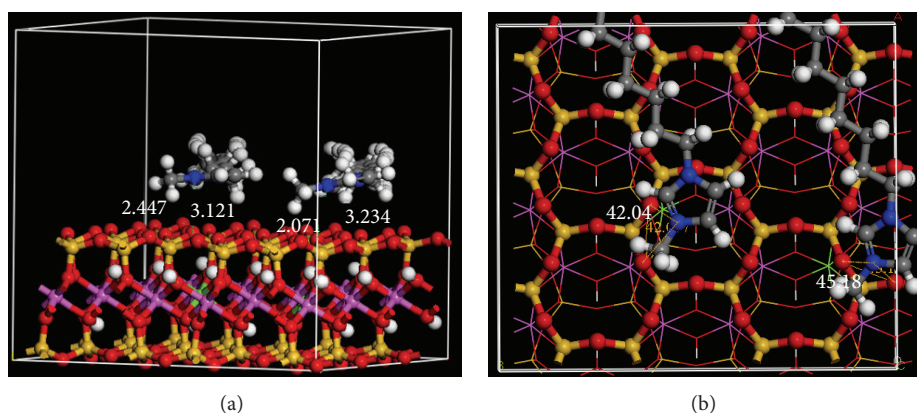

(a)

(b)

FIGURE 7: Molecular dynamic simulation of the distance (a) and angle (b) of C_{12}mim$^+$ and $[SiO_4]$.
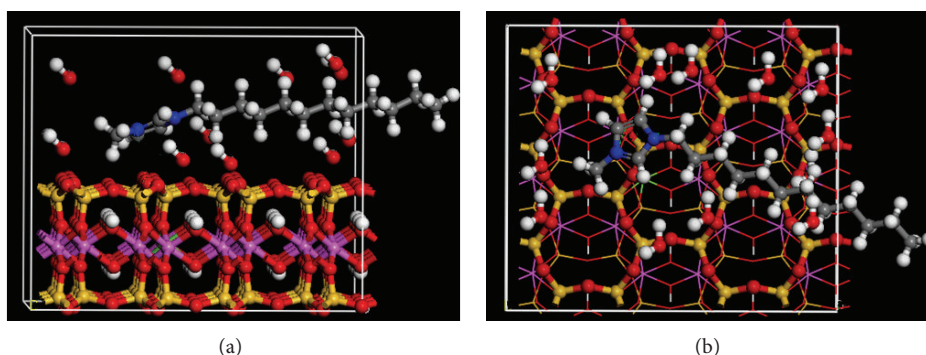

(a)

(b)

FIGURE 8: Molecular dynamic simulation of the distance of C_{12}mim$^+$ with $[SiO_4]$.

intercalation process. The intercalation processes were rapid and could reach the equilibrium in 5 min. Overall results confirmed that for different amount of organic loading, the interlayer organic carbon would have a different configuration, including lateral monolayers, lateral bilayers, and paraffin structure. They were in agreement with previous observations. The mechanisms of C_{12}minCl intercalation to Mt interlayer were electrostatic attraction and intermolecular force. The amount of intercalation affected application parameters of composite material, such as viscosity, contact angle, and thixotropic loop area. This composite material was a kind of environmentally friendly organic clay composite and could be used in drilling fluid system.

Conflict of Interests

The authors declare that there is no conflict of interests regarding the publication of this paper.

Acknowledgments

References

[1] M. Ogawa, *Photoprocesses in Clay-Organic Complexes*, Marcel Dekker, New York, NY, USA, 2004.

[2] G. Lagaly, M. Ogawa, and I. Dékány, *Clay Mineral Organic Intercalation*, Elsevier, Amsterdam, The Netherlands, 2006.

[3] N. Khaorapapong, A. Ontam, J. Khemprasit, and M. Ogawa, "Formation of MnS- and NiS-montmorillonites by solid-solid reactions," *Applied Clay Science*, vol. 43, no. 2, pp. 238–242, 2009.

[4] N. Khaorapapong and M. Ogawa, "Solid-state intercalation of 8-hydroxyquinoline into Li(I)-, Zn(II)- and Mn(II)-montmorillonites," *Applied Clay Science*, vol. 35, no. 1-2, pp. 31–38, 2007.

[5] N. Khaorapapong, A. Ontam, and M. Ogawa, "Formation of ZnS and CdS in the interlayer spaces of montmorillonite," *Applied Clay Science*, vol. 50, no. 1, pp. 19–24, 2010.

[6] W. Dye, K. d'Augereau, N. Hansen et al., "New water-based mud balances high-performance drilling and environmental compliance," in *Proceedings of the SPE/IADC Drilling Conference*, SPE/IADC Paper 92367, pp. 23–25, Amsterdam, The Netherlands, 2006.

[7] C. Gatlin, *Petroleum Engineering: Drilling and Well Completions*, Prentice-Hall, Englewood Cliffs, NJ, USA, 1960.

[8] B. G. Chesser, "Design considerations for an inhibitive, stable water-based mudsystem," in *Proceedings of the IADC/SPE Drilling Conference*, SPE Paper 14757, pp. 10–12, Dallas, Tex, USA, 1987.

[9] V. C. Kelessidis, R. Maglione, C. Tsamantaki, and Y. Aspirtakis, "Optimal determination of rheological parameters for Herschel-Bulkley drilling fluids and impact on pressure drop, velocity profiles and penetration rates during drilling," *Journal of Petroleum Science and Engineering*, vol. 53, no. 3-4, pp. 203–224, 2006.

[10] S. Z. Jilani, H. Menouar, A. A. Al-Majed, and M. A. Khan, "Effect of overbalance pressure on formation damage," *Journal of Petroleum Science and Engineering*, vol. 36, no. 1-2, pp. 97–109, 2002.

[11] N. M. Soule and S. E. Burns, "Effects of organic cation structure on behavior of organobentonites," *Journal of Geotechnical and Geoenvironmental Engineering*, vol. 127, no. 4, pp. 363–370, 2001.

[12] S. E. Burns, S. L. Bartelt-Hunt, J. A. Smith, and A. Z. Redding, "Coupled mechanical and chemical behavior of bentonite engineered with a controlled organic phase," *Journal of Geotechnical and Geoenvironmental Engineering*, vol. 132, no. 11, pp. 1404–1412, 2006.

[13] B. Bate and S. E. Burns, "Effect of total organic carbon content and structure on the electrokinetic behavior of organoclay suspensions," *Journal of Colloid and Interface Science*, vol. 343, no. 1, pp. 58–64, 2010.

[14] A. Z. Redding, S. E. Burns, R. T. Upson, and E. F. Anderson, "Organoclay sorption of benzene as a function of total organic carbon content," *Journal of Colloid and Interface Science*, vol. 250, no. 1, pp. 261–264, 2002.

[15] I. M.-C. Lo, "Organoclay with soil-bentonite admixture as waste containment barriers," *Journal of Environmental Engineering*, vol. 127, no. 8, pp. 756–759, 2001.

[16] J. A. Smith and P. R. Jaffer, "Adsorptive selectivity of organic-cation-modified bentonite for nonionic organic contaminants," *Water, Air, and Soil Pollution*, vol. 72, no. 1–4, pp. 205–211, 1994.

[17] J.-W. Park and P. R. Jaffé, "Partitioning of three nonionic organic compounds between adsorbed surfactants, micelles, and water," *Environmental Science & Technology*, vol. 27, no. 12, pp. 2559–2565, 1993.

[18] G. Y. Sheng and S. A. Boyd, "Relation of water and neutral organic compounds in the interlayers of mixed Ca/trimethyl-phenylammonium-smectites," *Clays and Clay Minerals*, vol. 46, no. 1, pp. 10–17, 1998.

[19] R. J. Lorenzetti, S. L. Bartelt-Hunt, S. E. Burns, and J. A. Smith, "Hydraulic conductivities and effective diffusion coefficients of geosynthetic clay liners with organobentonite amendments," *Geotextiles and Geomembranes*, vol. 23, no. 5, pp. 385–400, 2005.

[20] J. Dupont, "On the solid, liquid and solution structural organization of imidazolium ionic liquids," *Journal of the Brazilian Chemical Society*, vol. 15, no. 3, pp. 341–350, 2004.

[21] J. Dupont, G. S. Fonseca, A. P. Umpierre, P. F. P. Fichtner, and S. R. Teixeira, "Transition-metal nanoparticles in imidazolium ionic liquids: recyclable catalysts for biphasic hydrogenation reactions," *Journal of the American Chemical Society*, vol. 124, no. 16, pp. 4228–4229, 2002.

[22] C. P. Mehnert, "Supported ionic liquid catalysis," *Chemistry—A European Journal*, vol. 11, no. 1, pp. 50–56, 2005.

[23] A. Riisager, R. Fehrmann, M. Haumann, and P. Wasserscheid, "Supported ionic liquids: versatile reaction and separation media," *Topics in Catalysis*, vol. 40, no. 1–4, pp. 91–102, 2006.

[24] P. Lozano, E. García-Verdugo, R. Piamtongkam et al., "Bioreactors based on monolith-supported ionic liquid phase for enzyme catalysis in supercritical carbon dioxide," *Advanced Synthesis and Catalysis*, vol. 349, no. 7, pp. 1077–1084, 2007.

[25] S. J. Chipera and D. L. Bish, "Baseline studies of the clay minerals society source clays: powder X-ray diffraction analyses," *Clays and Clay Minerals*, vol. 49, no. 5, pp. 398–409, 2001.

[26] D. Borden and R. F. Giese, "Baseline studies of the clay minerals society source clays: cation exchange capacity measurements by the ammonia-electrode method," *Clays and Clay Minerals*, vol. 49, no. 5, pp. 444–445, 2001.

[27] A. R. Mermut and G. Lagaly, "Baseline studies of the clay minerals society source clays: layer-charge determination and characteristics of those minerals containing 2:1 layers," *Clays and Clay Minerals*, vol. 49, no. 5, pp. 393–397, 2001.

[28] S. Azizian, "A novel and simple method for finding the heterogeneity of adsorbents on the basis of adsorption kinetic data," *Journal of Colloid and Interface Science*, vol. 302, no. 1, pp. 76–81, 2006.

[29] B. Klebow and A. Meleshyn, "Monte Carlo study of the adsorption and aggregation of alkyltrimethylammonium chloride on the montmorillonite-water interface," *Langmuir*, vol. 28, no. 37, pp. 13274–13283, 2012.

[30] S. Dultz, B. Riebe, and C. Bunnenberg, "Temperature effects on iodine adsorption on organo-clay minerals. II. Structural effects," *Applied Clay Science*, vol. 28, no. 1–4, pp. 17–30, 2005.

[31] J. Bors, S. Dultz, and B. Riebe, "Retention of radionuclides by organophilic bentonite," *Engineering Geology*, vol. 54, no. 1-2, pp. 195–206, 1999.

[32] R. L. Frost, Q. Zhou, H. He, and Y. Xi, "An infrared study of adsorption of para-nitrophenol on mono-, di- and tri-alkyl surfactant intercalated organoclays," *Spectrochimica Acta—Part A: Molecular and Biomolecular Spectroscopy*, vol. 69, no. 1, pp. 239–244, 2008.

[33] N. V. Venkataraman and S. Vasudevan, "Conformation of methylene chains in an intercalated surfactant bilayer," *The Journal of Physical Chemistry B*, vol. 105, no. 9, pp. 1805–1812, 2001.

[34] B. Ha and K. Char, "Conformational behavior of dodecyldiamine inside the confined space of montmorillonites," *Langmuir*, vol. 21, no. 18, pp. 8471–8477, 2005.

[35] R. A. Vaia, R. K. Teukolsky, and E. P. Giannelis, "Interlayer structure and molecular environment of alkylammonium layered silicates," *Chemistry of Materials*, vol. 6, no. 7, pp. 1017–1022, 1994.

[36] Y. Li and H. Ishida, "Concentration-dependent conformation of alkyl tail in the nanoconfined space: hexadecylamine in the silicate galleries," *Langmuir*, vol. 19, no. 6, pp. 2479–2484, 2003.

[37] Y. Xi, Z. Ding, H. He, and R. L. Frost, "Infrared spectroscopy of organoclays synthesized with the surfactant octadecyltrimethylammonium bromide," *Spectrochimica Acta—Part A: Molecular and Biomolecular Spectroscopy*, vol. 61, no. 3, pp. 515–525, 2005.

[38] H. Hongping, F. L. Ray, and Z. Jianxi, "Infrared study of HDTMA+ intercalated montmorillonite," *Spectrochimica Acta Part A: Molecular and Biomolecular Spectroscopy*, vol. 60, no. 12, pp. 2853–2859, 2004.

[39] K. Suga and J. F. Risling, "Structural characterization of surfactant and clay-surfactant films of micrometer thickness by FT-IR spectroscopy," *Langmuir*, vol. 9, no. 12, pp. 3649–3655, 1993.

[40] L. Wu, C. Yang, L. Mei, F. Qin, L. Liao, and G. Lv, "Microstructure of different chain length ionic liquids intercalated into montmorillonite: a molecular dynamics study," *Applied Clay Science*, vol. 99, pp. 266–274, 2014.

[41] H. Heinz, W. Paul, U. W. Suter, and K. Binder, "Analysis of the phase transitions in alkyl-mica by density and pressure profiles," *Journal of Chemical Physics*, vol. 120, no. 8, pp. 3847–3854, 2004.

[42] H. Heinz, H. J. Castelijns, and U. W. Suter, "Structure and phase transitions of alkyl chains on mica," *Journal of the American Chemical Society*, vol. 125, no. 31, pp. 9500–9510, 2003.

Journal of
Nanotechnology

International Journal of
Corrosion

International Journal of
Polymer Science

Smart Materials
Research

Journal of
Composites

BioMed
Research International

Journal of
Metallurgy

Journal of
Materials

Hindawi

Submit your manuscripts at
http://www.hindawi.com

Journal of
Nanoparticles

Advances in
Materials Science and Engineering

Scientifica

Journal of
Nanomaterials

The Scientific
World Journal

International Journal of
Biomaterials

Journal of
Nanoscience

Journal of
Coatings

Journal of
Crystallography

Journal of
Ceramics

Journal of
Textiles